Back analysis of a landslide in a residual soil slope in Rio de Janeiro, Brazil

D. M. S. GERSCOVICH

Civil Engineering Department, State University of Rio de Janeiro, Brazil

T. M. P. DE CAMPOS AND E. A. VARGAS JR

Civil Engineering Department Pontifical Catholic University of Rio de Janeiro, Brazil

ABSTRACT

After a short period of relatively intense rainfall, a deep-seated landslide occurred in a slope in Rio de Janeiro. The mass movement buried cars, and caused structural damages to an adjacent building. The exposed failure surface was completely saturated, regardless of the inexistence of groundwater within the slope. At this site, a comprehensive laboratory and field investigation was undertaken to determine the hydro-geotechnical parameters of the residual soil profile. Numerical modeling of infiltration processes revealed that the rainfall amount was insufficient to reproduce the saturation condition of the failure surface. On the other hand, this critical condition could be rapidly achieved if the numerical analysis incorporated the changes of slope geometry, due to the displacement of the soil mass above the failure surface, or the development of a preferential infiltration path through the fractured soil-rock layer transition.

This paper evaluates the influence of the different scenarios that were conceived for the simulations of the infiltration processes in the stability of the slop. The geotechnical parameters used in the stability analyses were defined according to laboratory shear test carried out on samples extracted from the slide surface and from an undisturbed location of the slope. Pore pressure distributions at the central section of the landslide were obtained from previous results of flow simulations.

Factors of safety were computed for the actual failure surface and for the one with the minimum factor of safety. Regardless of the geometry of the failure mass, the stability analyses indicated the landslide could not be triggered solely by rain infiltration. Amongst various alternatives, the

existence of a preferential flow through a fractured layer of the bedrock revealed to be the only feasible scenario that could reproduce not only the saturated condition, but also a factor of safety close to 1.

Deep-seated landslides of unsaturated residual slopes are relatively common in tropical countries. Despite the usual approach of identifying the landslide as a rainstorm-induced mechanism, it appears to be more complex and other infiltration sources may play an essential role.

Keywords: unsaturated soil, stability analysis, transient flow, residual soil

1. Introduction

Rio de Janeiro city is located in the southeastern region of Brazil. Its mountainous relief associated to a tropical humid climate results in slopes of unsaturated residual soil with thickness that may vary from few centimeters to dozen of meters. Rain-induced soil and/or rock mass movements are quite frequent, during or immediately after periods of intense rainfall.

Despite of the considerable progress in the understanding of the behavior of unsaturated soils, it is actually very difficult to predict when or where a landslide may happen. Nevertheless, it is recognized that rainfall-induced landslides are caused by changes in pore water pressures.

Many authors have attempted to address the likely causes of landslides (e.g. Kim et al., 2004; Capra et al, 2003; Gasmo et al, 2000; Au, 1998; Costa Nunes et al, 1989; Wolle and Hachich, 1989; Vargas et al, 1986). Shallow failures may be attributed to the deepening of a wetting front into the slope, which results in a decrease of matric suction or to the development of the weathering process of steep slopes. Large landslides and debris flows usually result from the development of positive pore pressures that comes along with fully saturation of the soil mass. This scenario may be achieved when infiltrating water encounters a low permeability soil layer and a transient perched water table occurs (Capra et al, 2003) or when water infiltrates through fractured layers of the bedrock (Dietrich et al, 1986; Wilson, 1988; Vargas Jr. et al, 1990). Further studies have also

illustrated that positive pore pressure generation along the failure surface may be produced by the crushing of soil grains resulting in a liquefied soil condition (Wang and Sassa, 2003) or as a consequence of soil contraction that originates at the sliding surface and spreads to the unsaturated soil mass (Capra et al, 2003).

In February 1988, a considerable number of soil/rock slides occurred in various slopes in Rio de Janeiro city. Most of them were shallow and quite long in extension (100-150m) and were classified as being amongst the largest that have occurred in the city. The pluviometric data corresponding to 21 days indicated an accumulated amount of 515.6mm, with a rain peak of 85.4mm in a single day.

Nine months later, in November, a deep-seated slide occurred in a re-vegetated slope (Figure 1) after a period of a medium intensity rainfall. After 21 days, the accumulated rainfall amount was 246.3mm, with a maximum rain peak of 57.5mm. The failure caused structural and material damages to an adjacent building, with the shearing of one pillar and complete destruction of one apartment. Several cars in external and internal building parking areas were also damaged. Fortunately, nobody was injured. Despite no evidence of groundwater within the slope, on the following day and continuously for the following week after the slide, there were clear indications of full saturation of the failure surface, with groundwater springs at its upper region.

(a) day after photo

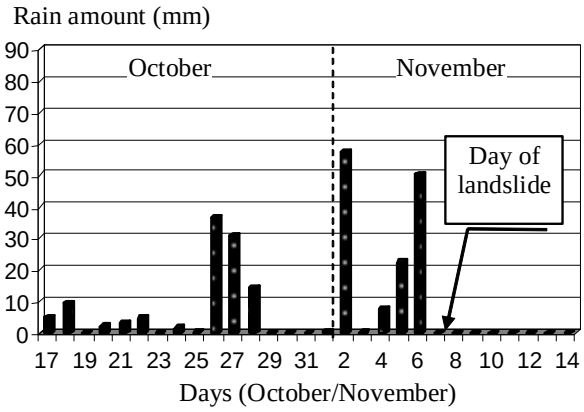

(b) daily rain amount

Figure 1. Slope view and pluviometric data.

Figure 2 shows a schematic topographic plan of the site before the landslide. The slope crest shows a maximum elevation of 384m and surface inclinations ranging from 30^{o} to 55°. At the toe of the slope there was a gravity wall aligned with an anchored wall, located at the rear of the Building A. The superficial drainage system, located at the upper region of the slope, was presumably

malfunctioning, since blockage of the channel adjacent to the slide was observed during field inspections.

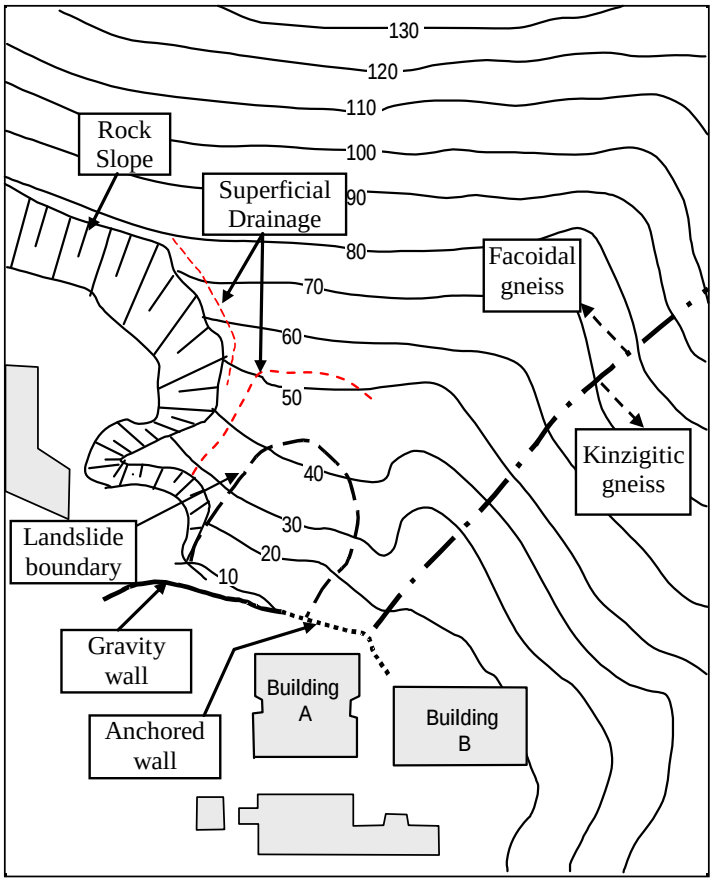

Figure 2. Schematic site plan before landslide.

Preliminary analyses disregarded the hypothesis of failure of the retaining wall structure as the shape of the failure surface suggested a major tendency of soil movement over the wall crest. There was also no evidence that the accumulated rainfall could have raised the water table, which was located at a considerable depth below ground level. Using a simple one-dimensional water balance, one can prove that a large amount of water would be required to achieve soil saturation. Considering the average depth of the sliding mass to be approximately 5m, fully drained condition and antecedent porosity and volumetric water content corresponding to 0.38 and 0.1, respectively, full saturation of the profile would require at least 1400 mm of infiltrating water. Moreover, the amount that infiltrates depends, among other factors, on the contrast of the rainfall rate and saturated hydraulic conductivity, slope topography, vegetation, etc. Consequently, the amount of

infiltration would be less than the values predicted by the pluviometers data. Nevertheless, the triggering mechanism was undoubtedly associated to changes in the pore water pressure and it was likely that complex changes of the slope hydrogeology might have occurred.

Numerical 3D-FEM transient flow analyses were carried out to identify the infiltration process that could explain field evidence of complete saturation of the failure surface. Different boundary conditions were conceived and the results revealed that only major changes of the slope hydrogeology could justify the deep-seated slope failure (Gerscovich et al, 2006).

This paper describes the experimental programme, presents field and laboratory results regarding geotechnical parameters of the residual soil and the uses the slope stability approach to verify the validity of the previously obtained results of flow simulations.

2. Geotechnical Investigation

A comprehensive series of field and laboratory tests was carried out to determine soil profile and geotechnical and hydrological parameters.

Field investigation comprised seismic refraction surveys, percussion and rotary drillings. They indicated a varying thickness profile of unsaturated residual soil, originated from a gneissic metamorphic rock that outcropped at the upper and left sides of the landslide boundary.

The residual soil layer showed depths varying from 0m to 15m. The weathering profile was composed of a superficial mature clayey sand residual soil, with an average thickness of 1m, underlain by a layer of a sandy matrix young residual soil (saprolitic soil), with a well defined inherited mineral alignment from the parent rock. The transition between the sound rock and the saprolitic soil is a highly fractured and weathered rock with a thickness varying within 4 to 10m. The mechanical soundings did not indicate the presence of a groundwater level within the soil mass. However, water level was observed in some rotary drillings within the fractured rock layer. Figure 3 shows a typical soil profile of the instrumented area.

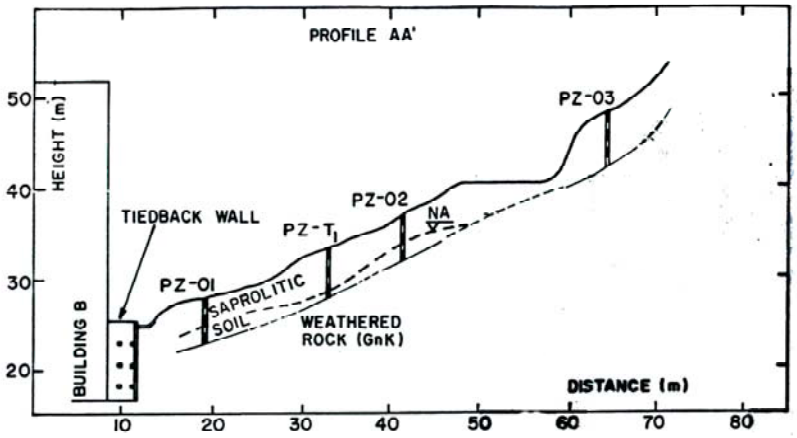

Figure 3. Soil profile at the instrumented area.

Field instrumentation was installed outside the slide area and consisted of piezometers, inclinometer tubes and a pluviometric station. Maxima piezometers (Brand, 1985) were also installed at the soil-rock interface to record maximum transient water pressure levels. More details regarding field instrumentation refer to Gerscovich et al (2006).

Topographic plants that were generated before and after the slide, aerophotos taken between 1966 and 1975, and logging profiles were used to restore the original geometry of the whole area and to define the landslide surface, as well. The failure surface presented an ellipse shape with the relationship width (perpendicular to the movement) and length (in the direction of the movement) of approximately 0.6. Figure 4 displays the reconstructed 3D geometry of the hillside and a view of the 2D central section of the slope.

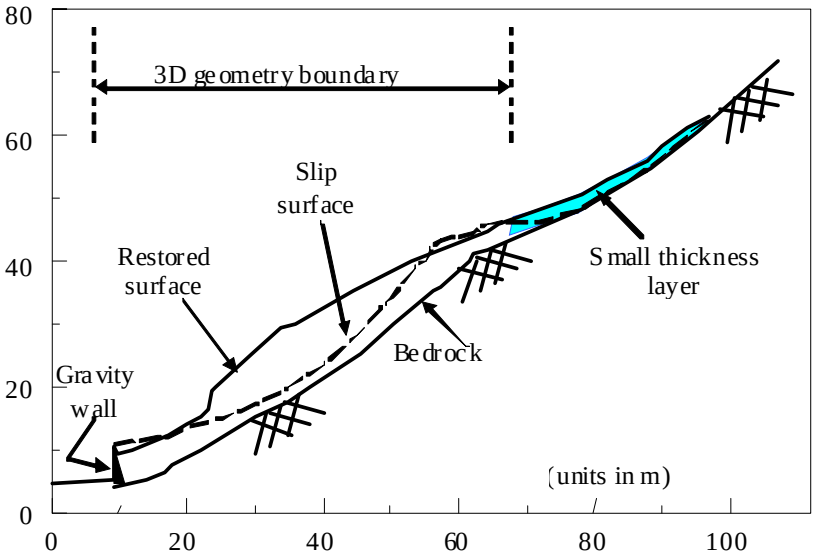

(a) Central section

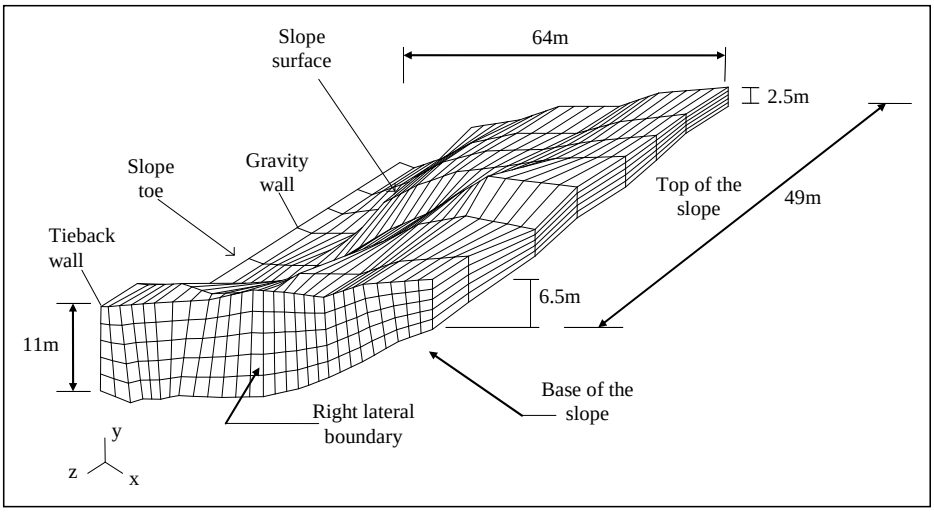

(b) 3D view (without upper small thickness layer)

Figure 4. Restored geometry

Block samples were extracted from slope failure surface and from a trench located 50m away from the failure zone. The laboratory investigation comprised geotechnical characterization, determination of hydraulic parameters (hydraulic conductivity and water retention curve) and shear strength tests.

2.1. Soil Characterization

Table 1 shows a summary of the characterization tests with the average physical indexes. Two different materials appeared at the failure surface: an apparently homogeneous and isotropic red-

colored mature residual soil, and a grey saprolitic soil, with a well-defined mineral alignment. At the trench, only the saprolitic soil was extracted and it was coarser and denser than the one from the slip surface.

Table 1. Soil characterization

Location	Slip surface		Trench
Soil type	Saprolitic soil	Mature soil	Saprolitic soil
Sand (%)	63.0	56.0	82.0
Silt (%)	27.5	34.0	9.8
Clay (%)	9.5	10.0	8.2
ω_L (%)	38.2	39.5	-
ω_P (%)	NP	24.7	-
ω (%)	19.0	21.2	6.4
θ (%)	22.4	25.5	10.3
G_s	2.64	2.63	2.66
e	1.19	1.14	0.62
n	0.54	0.53	0.38
γ_t (kN/m^3)	14.0	14.6	17.1

Notes: ω_L= liquid limit; ω_L = plasticity limit; ω = water content; θ = volumetric water content; G_s = specific gravity of grains; e= voids ratio, n = porosity, γ_t = in situ density

The volumetric soil moisture profile of the saprolitic soil extracted from the trench, located behind Building B, is shown in Figure 5. The results indicated volumetric water content around 25% on the surface and a gradual reduction with depth. Below 2m depth, this value is approximately constant and equal to 9%.

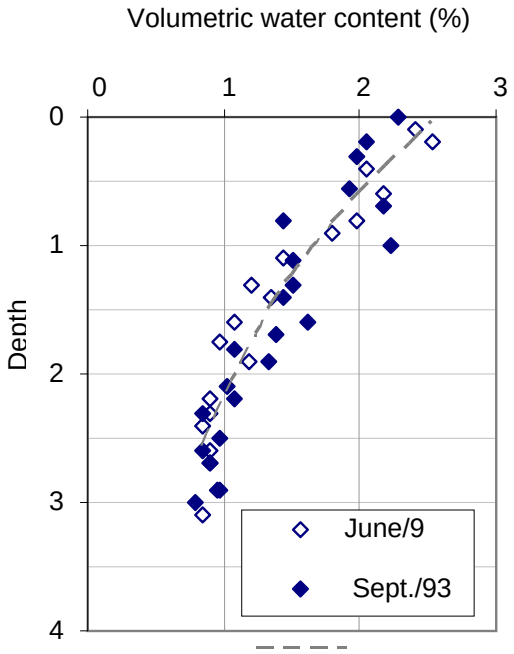

Figure 5. Volumetric water content profiles of the saprolitic soil from the trench.

2.2. Shear Strength Parameters

Isotropically consolidated drained triaxial tests (CID) were performed on saturated 100mm-diameter undisturbed samples of the saprolitic soil extracted from the trench. The specimens were molded with the xistosity plane inclined around 30^{o} with the horizontal plane. The consolidation stress levels ranged from 25 to 200kPa and the shearing velocity was 0.0122mm/min. The triaxial chamber allowed the use of internal devices for automatic measurement of axial and radial strains and volume changes (water and total volume). The variations of air volume were mechanically monitored by a bubble trap device (Aguilar, 1990).

Conventional direct shear tests were carried out on soil samples extracted from the slip surface. The saprolitic soil specimens were molded with the shearing plane parallel and perpendicular to the plane of xistosity. In spite of the apparent isotropic condition, the mature soil samples were also prepared according two perpendicular angles. The samples were initially saturated, prior to the consolidation stage, under normal stresses ranging from 22 to 135kPa. The shearing velocity was 0.0036mm/min and the shear box was prepared with an opening of 0.5mm.

Figure 6 shows the shear strength test results of the saprolitic soil and Table 2 summarizes the mean values of strength parameters, since no influence of the shear plane angle with respect to the xistosity orientation has been observed. The results revealed a reasonable agreement between the direct shear and the triaxial tests of the saprolitic soil, despite the differences on soil characterization.

The Mohr-Coulomb strength envelope of the saprolitic soil could be fitted by a straight line with effective cohesion and friction angle equal to 13kPa and 33^{o}. However, due to the relatively high percentage of sand, it would be expected a null cohesion within the range of low confining stresses. For that reason, the Mohr-Coulomb strength envelope would better defined by a bi-linear curve that is also plotted in Figure 6.

Table 2. Saturated Strength Parameters

Test	Conventional Direct Shear test		Triaxial test
Soil	Saprolitic soil	Mature soil	Saprolitic soil
c'(kPa)	14.6	4.8	9.6
$\phi'(^{o})$	31.8	27.5	34.0

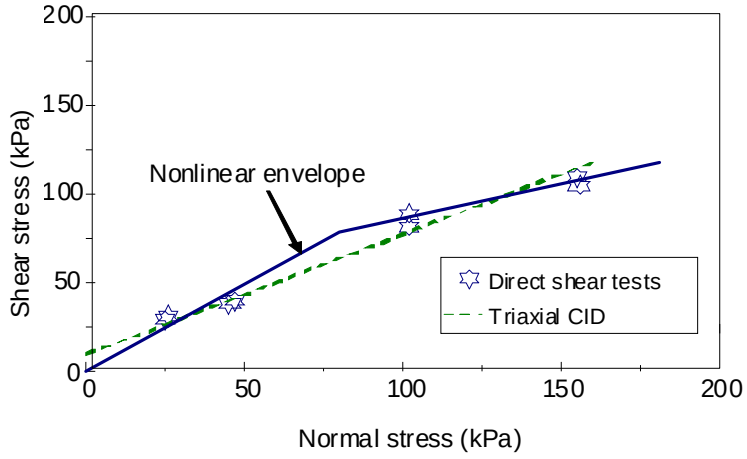

Figure 6. Shear strength of saprolitic soil – saturated condition

The small thickness mature residual soil provided lower values of strength parameters as a result of a more intense weathering process.

The shear strength response of the residual soil under unsaturated condition was determined by direct shear tests with suction control. The tests were carried out on samples extracted from the slip surface, according to a multi stage technique (Ho and Fredlund, 1982), following the wetting path (Fonseca, 1991; Carrillo et al 1994). Similarly to the saturated tests, specimens were molded with shearing plane parallel and perpendicular to the plane of xistosity. The samples were initially consolidated to a vertical stress of 50kPa, and then submitted to decreasing suctions from 200 to 15kPa (de Campos et al, 1994). The shearing velocity was 0.0366mm/min.

The shear strength of unsaturated soils is based on the Mohr-Coulomb criterion and, according to Fredlund et al (1978), can be expressed by:

$$\tau = c' + (u_a - u_w) tg\phi^b + (\sigma - u_a) tg\phi' \qquad (1)$$

where, u_a and u_w are the pore air and pore water pressure, respectively, σ is the total normal stress; c' and ϕ' are effective strength parameters and ϕ^b is the angle indicating the rate of increase in shear strength relative to the matric suction. ϕ^b is equal to ϕ' at low matric suction, and decreases to a lower value at high matric suctions (Teknsoy et al, 2004).

Figure 7 shows the shear strength results with respect to soil suction. Similar to the saturated soil response, no influence of xistosity plane on the soil strength has been observed. The nonlinear relationship between the shear strength and soil suction was fitted by a bi-linear curve with $\phi^b = 33^o$, for soil suction up to 115kPa, and equal to 20^o, for higher values. For low soil suctions values, ϕ^b value was equivalent to ϕ'.

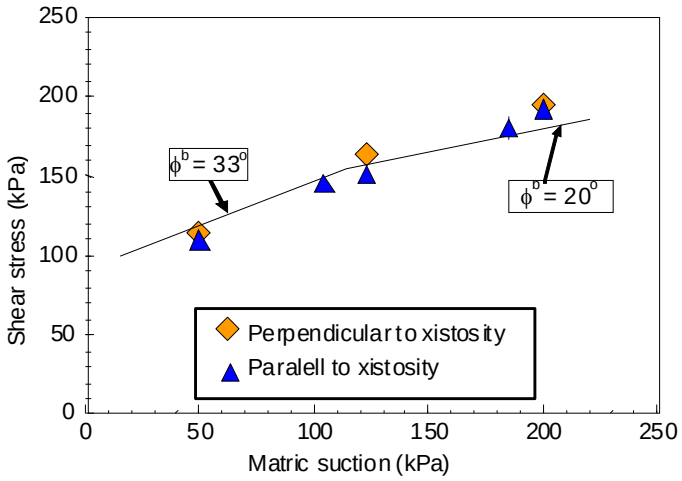

Figure 7. Unsaturated strength envelope

The similarity between ϕ^b and ϕ', for low values of matric suction, was also observed by Rahardjo et al (1995) in triaxial tests on residual soils of Singapore. Following a drying path, the authors obtained ϕ^b equal to 26^o, for matric suctions up to 400kPa, which was equal to the effective friction angle ϕ'.

It is worth to note that the relatively high ϕ^b values revealed the strong influence of the matric suction on the shear strength; any infiltration process promotes a substantial reduction of the shear strength.

2.3. Hydraulic Parameters

The hydraulic conductivities profiles were obtained in the laboratory with 100mm-diameter samples and in the field by means of Guelph permeameter tests (Reynolds and Elrick, 1987). The results, shown in Figure 8, reveal the changes of the hydraulic conductivity with depth within the first 3m of the soil profile, where there is a sharp decrease of k_{sat}. Below this depth, the hydraulic conductivity parameters were considered constant.

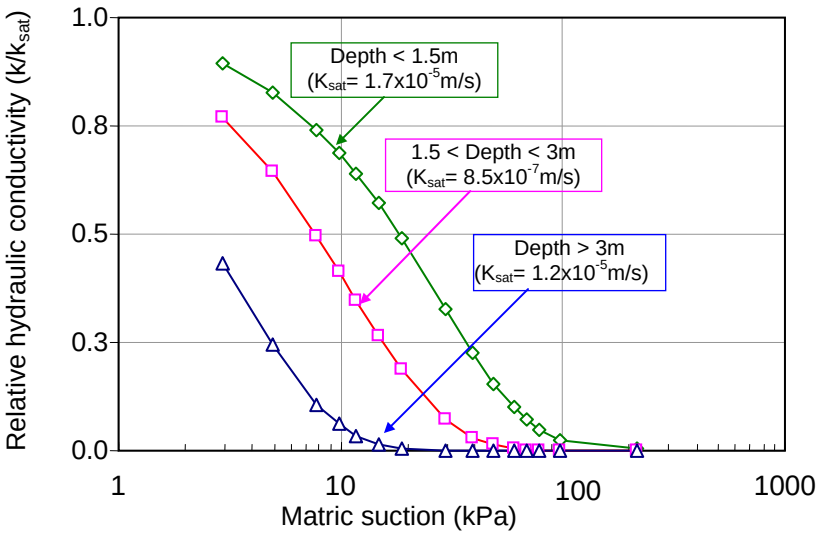

Figure 8.Prescribed relative hydraulic conductivity curves.

Soil-water retention curves (SWRC) were obtained on the saprolitic soil samples from the slip surface, following drying and wetting paths. The results, shown in Figure 9, indicated no significant deviation between the wetting and drying curves. A more detailed description regarding the hydraulic parameters tests and data interpretation are presented in Gerscovich et al (2006).

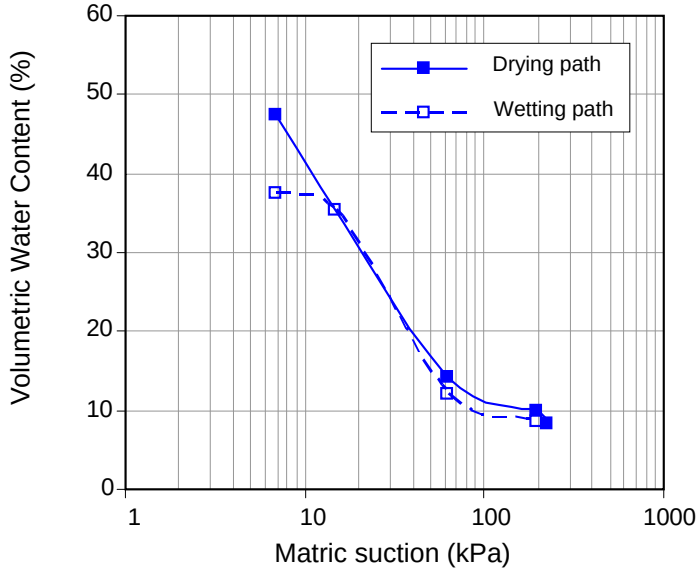

Figure 9. Soil-water retention curve of the saprolitic soil from the slip surface.

3. Transient Flow Simulations

The numerical modelling was carried out with FLOW3D computer program (Gerscovich, 1994) that solves 2D or 3D steady-state/transient flow through saturated-unsaturated soil. The mathematical development of the flow equation, built-in in the FLOW3D code, assumes that: i) flow is laminar and Darcian; ii) inertial forces, velocity heads, temperature gradients and chemical concentration gradients are all negligible; iii) soil is linearly elastic and isotropic; iv) hydraulic properties are not affected by volume changes; v) the air phase is continuous and always in connection with the constant, external atmospheric pressure; vi) the hysteretic behaviour of the SWRC is negligible; vii) the effect of soil compressibility on the storage of water under unsaturated conditions is quite small.

3.1. Slope geometry and Boundary conditions

The 3D mesh was composed by 1820 elements and 2436 nodes, as shown (Figure 4b). The small thickness layer, located at the top of the slope, was disregarded in order to avoid excessive mesh discretization. However, in some analyses, its effect was indirectly incorporated by prescribing pressure heads at nodes located at the top boundary.

The lateral boundaries, bottom of the slope, as well as the slope toe were considered as impervious surfaces. At the slope surface, daily rainfall events were simulated by prescribing flow velocities at the surface nodes, according to the amounts registered at a pluviometric station, located 4km away from the slope

The time dependent characteristic of the transient flow through unsaturated soil requires the knowledge of the antecedent distribution of matric suction (or soil moisture), previous to the simulation period. Flow modeling assumed null suction at the slope surface and a progressive increase of matric suction with depth. Below 2m-depth the soil suction was taken as constant and equal to 200kPa. These values were assumed by evaluating both the water content profile of the saprolitic soil (Figure 5) and the soil water retention curve (Figure 9).

3.2. Flow simulation results

Different scenarios of flow infiltration have been analyzed in an attempt to reproduce the full saturation of the slope that was observed the day after the landslide, despite the inexistence of groundwater within the soil mass (Gerscovich et al, 2006).

3.2.1 Case 1: Flow pattern predicted after 21 days of rainfall recorded in February, 1988.

The influence of rainfall intensity was initially evaluated by analysing flow patterns considering a more intense rainfall that occurred few months before the landslide. In this period, the accumulated rainfall was approximately 2 times greater than the registered in November, 1988, prior to the landslide. The results, shown in Figure 10, indicated slight changes in pressure head distributions, but no development of positive pore pressures within the soil slope. This pore-water pressure distribution is in disagreement to field observation after the landslide and suggests that rain infiltration solely would not be sufficient to produce significant pore-water changes.

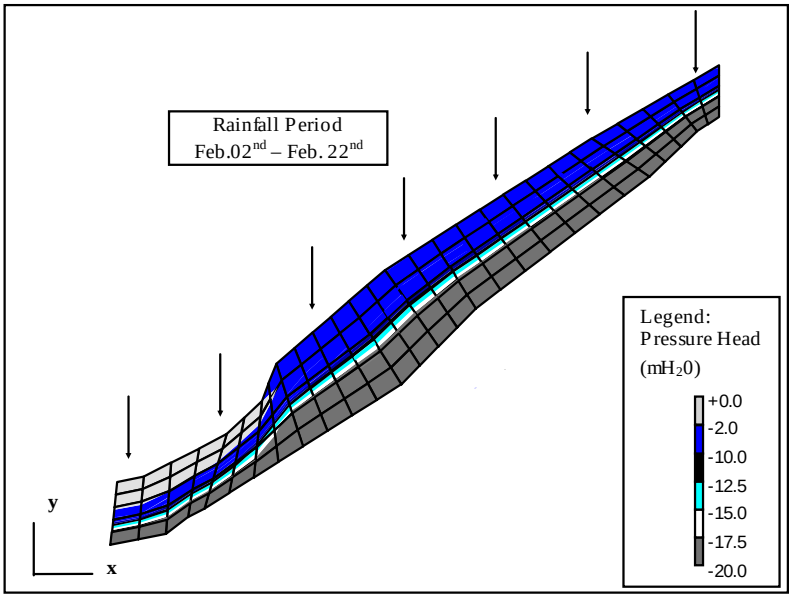

Figure 10. Pressure head distribution at central section - Case 1

3.2.2 Case 2: Flow pattern predicted after 19 days of rainfall recorded in November, 1988, with an extra pressure head imposed at the top of the slope

The effect of disregarding the small thickness layer, located at the top of the slope, was evaluated by analysing its response to rain infiltration. Thus, a 2D flow analysis of this varying thickness layer was carried out and revealed that 17 days of rainfall, prior to November 2nd (landslide day), could easily induce its complete saturation. In this study, the antecedent matric suction was set constant and equal to 10kPa, the lower and bottom boundaries were impervious and null pressure heads were prescribed at the upper boundary.

The effect of the saturation of the upper layer was incorporated in the 3D numerical analysis by prescribing hydrostatic pressure heads at the top boundary nodes. In this study, flow velocities imposed at the nodes of the slope surface comprised 19 days of rain events, from October 19th to November 7th. Figure 11 presents the pressure head distribution predicted at the central section of the slope. Despite the generation of positive pore pressure at the upper zone, mainly due to the progress of a saturation front, this result still did not reproduce the saturation condition of the failure surface that was verified after the slide.

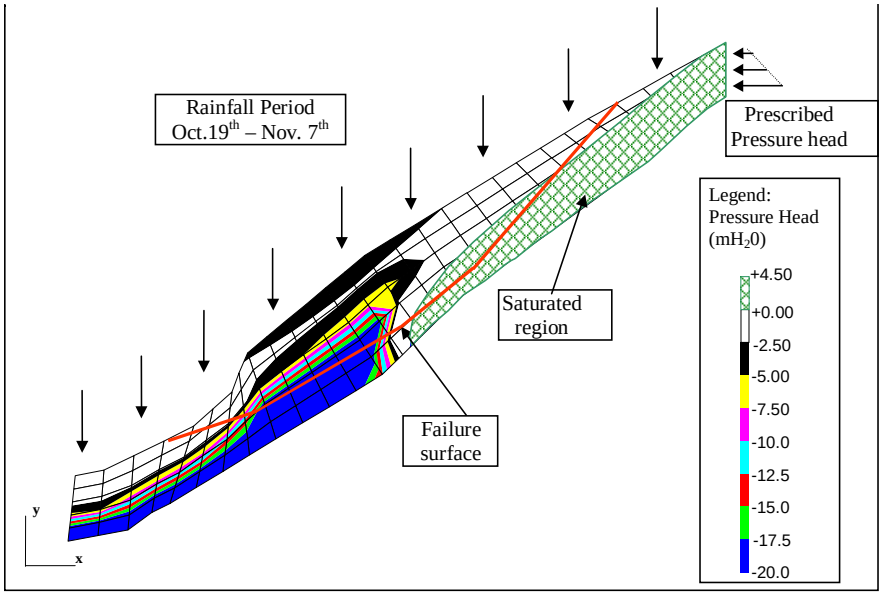

Figure 11. Pressure head distribution at central section - Case 2

An additional numerical analysis was carried out in an attempt to evaluate if geometry changes of the slope, produced by the displacement of the soil mass after the landslide, could accelerate the progression of the saturation front. This hypothesis was tested by performing a 2D numerical simulation of the central section of the slope, including the small thickness layer, located at the top of the slope. In this analysis, a high value of saturated hydraulic conductivity (k_{sat} = 1) was used for the soil above the failure surface and null pressure heads were prescribed at the nodes at failure surface. The antecedent moisture conditions where equivalent to the ones predicted after 19 days of rain simulation (Figure 11) and the remaining boundary conditions were unchanged. The results confirmed that few hours were sufficient to nearly cause a saturation of the whole soil mass and could be a feasible explanation for the saturation condition of the failure surface. However, it could not explain the landslide, since it was likely that large positive pore-water pressures would be required to reduce shear strength and cause the soil mass to fail.

3.2.3 Case 3: Flow pattern generated by a rainfall period of 5 days prior to the landslide and pressure heads prescribed at the top and at the base of the slope

Field investigations indicated the existence of a 4 to 10m thickness highly fractured rock layer at the transition of the sound rock and saprolitic soil. Maxima piezometers measured water levels restricted to this transition layer and confined to a small area.

The major role of the bedrock in generating high pore-water pressures have already been pointed out by other researchers (Dietrich et al, 1986; Wilson, 1988; Vargas Jr. et al, 1990).On the other hand, in the current engineering practice, it is very difficult not only to identify the existence of layers with high transmissivities but also to conceive an adequate mathematical model.

Nevertheless, the influence of an eventual preferential flow through the fracture systems was roughly evaluated by prescribing positive pressure heads at 13 nodes, located along a transversal line of nodes at the base of the 3D mesh, as shown in Figure 12. At each node, the magnitude of pressure head was equivalent to the vertical distance between the node coordinate and the highest

point of the slope mesh. This simulation was carried out for a time of approximately 6 days, from November 2nd to November 7th. Boundary conditions and antecedent soil suction were similar to the ones used in the previous analysis. The numerical simulation (Figure 12) showed that the whole soil mass nearly reached full saturation, with high levels of positive pore pressure been achieved and confirmed the major influence of water sources when they occur at the base of the slope.

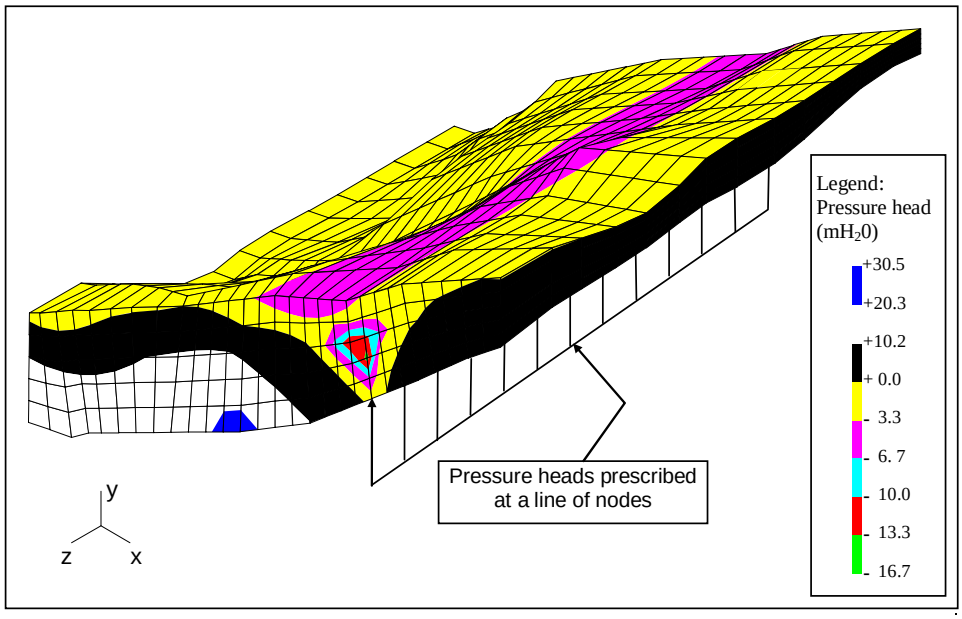

Figure 12. Pressure head distribution at central section - Case 3

4. Slope Stability Analyses

The stability analyses were carried out using the code SLOPE/W (GEO-SLOPE International Ltd), which allows for the computation of safety's factor, in 2D conditions.

The slope profile consisted of a superficial mature residual soil and a variable thickness saprolitic soil layer. Due to the small thickness of the mature residual soil, this layer was disregarded and the stability analyses were carried out considering a homogeneous material.

The geotechnical parameters were depicted from the laboratory tests and are listed in Table 3. The non-linearity of the effective strength envelope (Figure 6) was adjusted by two straight lines crossing at confining stress equal to 80kPa. Due to limitations of the computer program, the

unsaturated strength parameter (ϕ^b) was assumed constant and equal to the average value of the experimental results.

Table 3. Soil Parameters

Soil Parameter	Stress Level (kPa)	
	≤ 80.0	>80.0
γ_t (kN/m^3)	17,5	17,5
c´ (kPa)	0	44,2
ϕ' (°)	43,7	22
ϕ^b (°)	25	25

It is worthwhile to mention that the strength parameters correspond to peak values, as the stress-strain curves did not show any loss of strength for high strain levels.

The stability analyses were undertaken for the different scenarios of flow infiltration previously described. The pore-water pressure distributions at the central section of the slope were incorporated in the SLOPE/W program through a mesh of 46 nodes, as the program presents a limitation of the maximum number of nodes (50 nodes). The effect of pore air pressure was disregarded.

4.1. Case 1: Flow pattern predicted after 21 days of rainfall recorded in February, 1988.

Figure 13 displays the set of results of Morgenstern & Price method for a slip surface similar to the one observed in situ (FS=4.1) and for a potential failure surface derived from a grid of rotation centers (FS=3.5). The free search gave a lower factor of safety and the failure region was displaced upward. Nevertheless, both analyses provided high factors of safety.

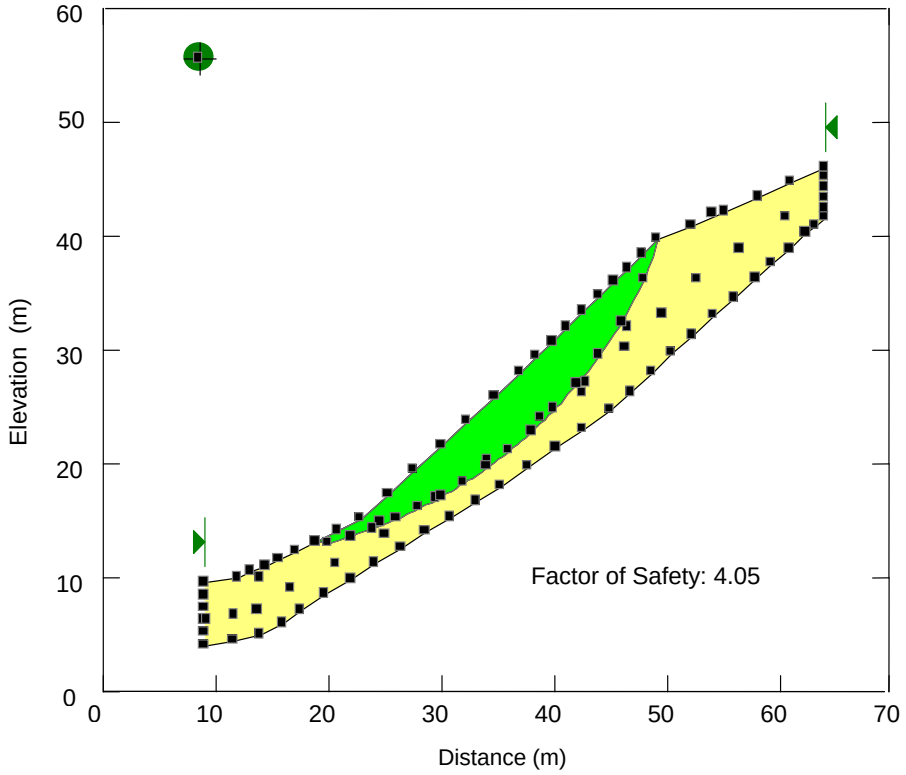

(a) Observed failure surface

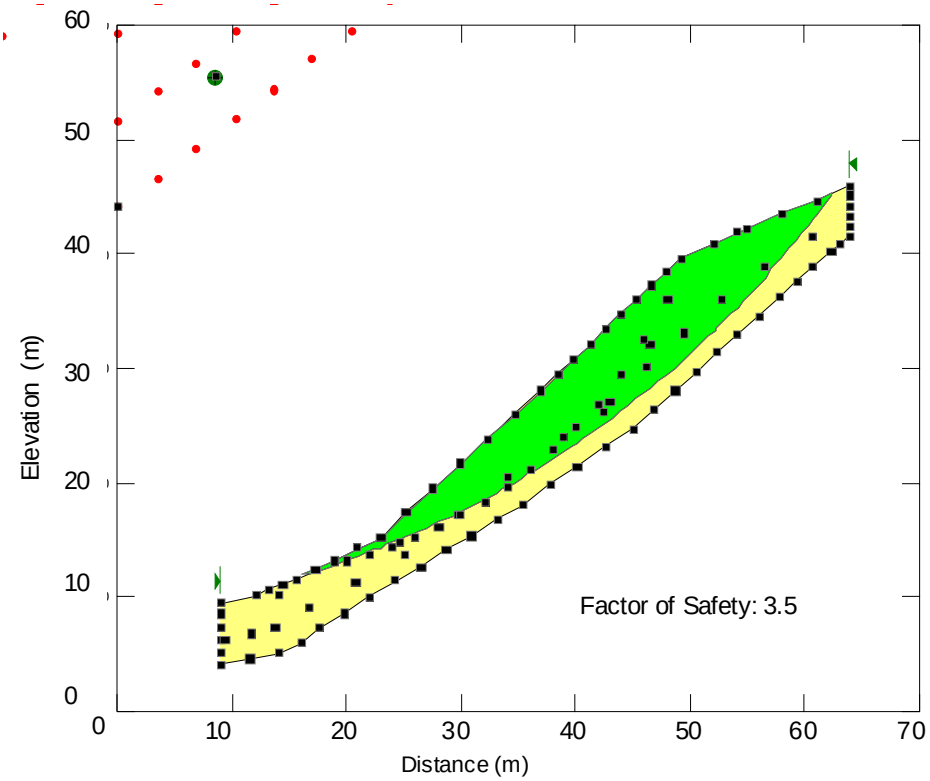

(b) Circular failure surface

Figure 13. Failure surfaces and Factors of Safety -Case 1

Shear tests with unsaturated samples indicated a bi-linear relationship between shear strength and matric suction and relatively high ϕ^b values. The influence of the matric suction on the was evaluated by performing analyses with ϕ^b =0. The results factors of safety were relatively high and equal to 1.53 and 1.67, for the circular search and field surfaces, respectively.

Stability analyses were also carried out in order to identify the likely range of shear strength parameters that would result in a FS close to 1. The smallest factors of safety (FS = 1.13 and 1.17, for the circular search and field surfaces, respectively) were computed by disregarding the influence of the matric suction and using the effective strength parameters obtained with the saturated CID tests.

It is worthwhile to emphasize that the analyses were carried out considering a plane strain condition. The 3D feature of the landslide would undoubtedly provide higher factors of safety.

The computed FS revealed that an ordinary amount of rain infiltration would not be sufficient to trigger the slope failure. These results are in accordance to the conclusions derived from the numerical simulations of rain infiltration, since it did not reproduce the saturated condition of the failure surface.

4.2. Case 2: Flow pattern predicted after 19 days of rainfall recorded in November, 1988, with an extra pressure head imposed at the top of the slope

The saturation of the small thickness layer, that could impose an additional boundary condition for water infiltration, was evaluated by prescribing pressure heads at the nodes located at the upper boundary of the slope. The alternative was based on the hypothesis of malfunctioning of the superficial drainage system, located above the landslide, causing saturation of the upper portion of the slope. The stability analyses with the corresponding pore water pressure mesh also revealed relatively high factors of safety, as shown in Figure 14.

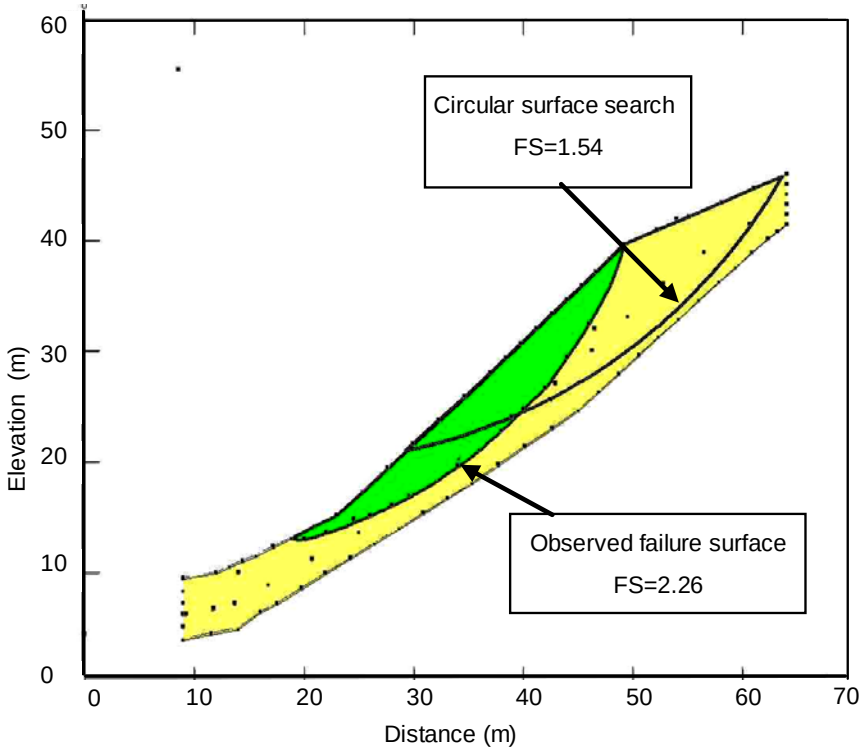

Figure 14. Failure surfaces and Factors of Safety - Case 2

4.3. Case 3: Flow pattern generated by a rainfall period of 5 days prior to the landslide and pressure heads prescribed at the top and at the base of the slope

Previous studies regarding the simulation of the flow pattern of the slope (Gerscovich et al, 2006) have pointed out that other mechanisms, other than rain infiltration over the slope surface, might played a major role on its hydrological pattern. The authors analyzed the influence of the development of a preferential flow through the fractures of the bedrock in generating pore pressure. The numerical simulation revealed that this scenario promoted an ideal condition for the landslide, since almost the entire slope achieved complete saturation. In fact, the slope stability analyses, shown in Figure 15, proved that this alternative could in fact explain the landslide. Due to its low FS, the analysis considering the field failure surface was aborted by SLOPE/W program.

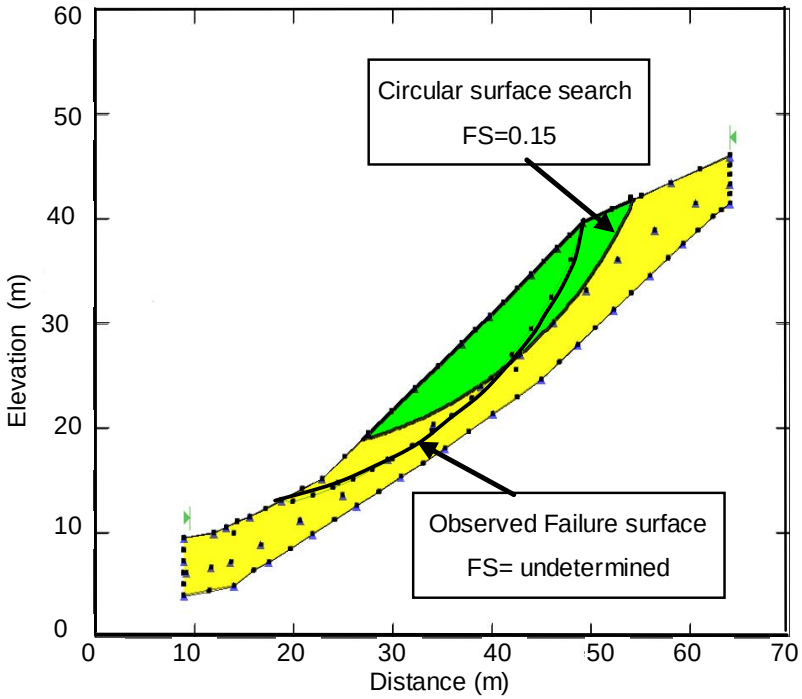

Figure 15. Failure surfaces and Factors of Safety - Case 3

5. Conclusions

A comprehensive experimental investigation and numerical analyses were undertaken in an attempt to identify the triggering mechanism of the deep-seated slide of a slope, in Rio de Janeiro, Brazil. The landslide occurred after a rainfall period and despite the unsaturated soil condition, field observations taken on the following day and even one week after the slide indicated full saturation of the failure surface, with groundwater sprouting at its upper region. Field investigations indicated a variable thickness unsaturated residual soil layer overlying a gneissic rock.

Despite the careful determination of the geotechnical and hydrogeological parameters and the use of a 3D-FEM transient/unsaturated flow program, the numerical simulation of the antecedent rainfall amount did not reproduce the saturation condition of the soil mass. As a result, other alternatives were evaluated in an attempt to assess the suitable condition that would promote the generation of positive pore-water pressure within the slope. The effect of the displacement of the soil mass above failure surface on the remaining soil, as well as the existence of a preferential flow

path though the fractured layer transition between the residual soil and the intact rock, revealed to be feasible scenarios that could explain the hydrological condition after the landslide.

This paper presented the back-analysis of the landslide focusing stability approach, which is much simpler than 3D saturated/unsaturated flow modeling and subjected to fewer uncertainties.

Triaxial and direct shear tests results, carried out on saturated samples extracted from the slip surface and next to the landslide, revealed a minor influence of grain alignment and that the shear strength parameters showed a reasonable agreement, despite the differences on the grain size distribution. The strength envelope was reasonably fitted by a bi-linear curve.

Controlled suction direct shear tests, on samples from the slip surface, were carried out following a wetting path. The soil the strength anisotropy could be disregarded, in agreement to the shear tests on saturated samples. The results suggested a bi-linear relationship between the unsaturated strength parameter (ϕ^b) and matric suction; ϕ^b was equal to 33^o, for low suction values (up to 115kPa), and reduced to 20^o, for higher values. This range is relatively high if compared to other residual soils and, therefore, implies in a significant shear strength reduction due to an infiltration process.

The stability analyses were carried out at the central section of the landslide, and FS were computed for the actual failure surface geometry and for the potential surface, computed after a free circular search. The numerical simulations of the different hydrological conditions were used to build the pore water pressure meshes.

The back-analysis of the landslide revealed a FS higher than 3.5, independent of the stability method and potential failure surface. This result implies that the rainfall amount that reached slope surface was insufficient to trigger slope failure and is also in agreement to flow simulations, since the predicted changes on matric suction were insufficient to produce a full saturation of the soil mass. As a result, stronger changes on the pore-water pressure would be required to achieve FS close to 1. The hypothesis of saturation of the failure surface due to the displacement of soil mass above failure surface became unlikely, as well.

The simulation of a preferential flow through the fractured region between the residual soil and the bedrock, in addition to the rainfall, resulted on a favorable condition to achieve the hydrological pattern observed on the site. In fact, the stability analyses proved that this alternative could be used to identify the main triggering mechanisms of the landslide

The results herein presented emphasize that, despite the development of experimental and numerical techniques to address the behavior of unsaturated soils, the understanding of the complex phenomenon of rainstorm-induced landslides is still a challenge among the geotechnical engineers. Besides, except for extreme and unpredictable rainfall amounts, landslides are triggered by a combination of mechanisms. Geotechnical engineers must call attention to the complexity of landslides in unsaturated residual soils, and always try to answer a simple question that many times arises: why the landslide did not occurred during a more intense event or why it did not occurred few meters away?

6. Acknowledgements

The authors acknowledge International Development Center (IDRC), Canada, and National Council for Research (CNPq) and FAPERJ, Brazil, for their financial support. The authors are also grateful to all graduate students that participated in this research project.

7. References

Au, S.W.C. 1998. Rain-induced slope instability in Hong Kong. Engineering Geology, 51(1), 1-36.

Brand, E.W. 1985. Geotechnical engineering in tropical residual soils. Proceedings of the 1st International Conference on Geomechanics in Tropical Lateritic and Saprolitic Soils, Brasília, Brazil, vol. 3, pp. 23-100.

Capra, L., Lugo-Hubp, J. and Borselli, L. 2003. Mass movements in tropical volcanic terrains: the case of Teziulán (Mexico) – Engineering Geology, 69 pp.359-379.

Carrillo, C.W.; Fonseca, E.C. & de Campos, T.M.P. 1994. Suction controlled direct shear device, 2nd Symposium on Unsaturated Soils, Recife, Brazil, pp 67-78 (in Portuguese).

Costa Nunes, A.J.; Couto Fonseca, A.M.M.C; Couto Fonseca, de M.; Fernandes, C.E. a& Craizer, W. 1989. Intense rainstorm and ground slides. Proceedings of the 12th Int. Conf. Soil Mech. and Foundation Engineering, vol.3, pp.1627-1630.

de Campos, T.M., Andrade, M.H.N, Gerscovich, D.M.S. & Vargas JR., E.A. 1994. Analysis of the Failure of an Unsaturated Gneissic Residual Soil Slope in Rio de Janeiro, Brazil - 1st. Pan American Symposium of Landslides - Guayaquil, Ecuador, vol.I, pp.201-213.

Dietrich, W.E.; Wilson, C.J. & Reneau, S L. 1986. Hollows, colluvium, and landslides in soil mantled landscapes. Hillslope Processes, edited by A.D. Abrahams, Allen & Unwin Ltd, pp.361-368.

Fonseca, E.C. 1991. Direct shear tests with suction control. MSc Thesis. Catholic University of Rio de Janeiro (in Portuguese).

Fredlund, D.G.; Morgenstern, N.R. e Widger, R.A. 1978. The Shear Strength of Unsaturated Soils - Canadian Geotechnical Jr., vol.15, pp 228-232.

Gasmo, J. M., Rahardjo, H. and Leong, E. C. 2000. Infiltration effect son stability of a residual soil slope – Computers and Geotechnics, 26, pp.145-165.

GEO-SLOPE International Ltd. SLOPE/W for slope stability analysis, version 5.0

Gerscovich D.M.S.; Campos T.P.P.; Vargas Jr E.A. 2006. On the evaluation of unsaturated flow in a residual soil slope in Rio de Janeiro Brazil. Engineering Geology. ISSN /0013-7952, v.88, p.23 - 40, 2006.

Ho, D.Y.F e Fredlund, D.G. 1982. The Increase in Shear Strength due to Soil Suction for two Hong Kong Soils - ASCE Geotechnical Conference on Engineering Construction in Tropical and Residual Soils, Honolulu, Hawaii, Janeiro, pp.263-295.

Kim, J. Jeong, S. Park, S. and Sharma, J. 2004. Influence of Rainfall-induced wetting on the

stability off slopes in weathered soils – Engineering Geology, 75, pp.251-262.

Rahardjo, H. ; Lim, T.T.; Chang, M.f. and Fredlund, D.G. 1995. Shear strength characteristics of a residual soil – Canadian Geotechnical Journal, 32, pp 60-77.

Reynolds, W.D. & Elrick, D.E. 1987. A laboratory and numerical assessment of the Guelph permeameter method. Soil Science144 (4), 282-292.

Tekinsoy, M. A.; Kayadelen, C.; Keskin, M.S.; Soylemez M. 2004. An equation for predicting shear strength envelope with respect to matric suction - Computers and Geotechnics, 31, pp 589-593

Vargas Jr., E. A.; Velloso, R.C., de Campos, T.M.P. & Costa Filho, L.M. 1990. Saturated-unsaturated analysis of water flow in slopes of Rio de Janeiro, Brazil. Computers and Geotechnics, 10 (3), 247-261.

Vargas Jr., E. A.; Costa Filho, L. M. & Prado Campos, L. E. 1986. A study of the relationship between stability of the slopes in residual soils and rain intensity. International Symposium on Environmental Geotechnology, ed. Fang. Envo, pp491-500.

Wang, G. and Sassa, K. 2003. Pore-pressure generation and movement of rainfall-induced landslides: effects of grain size and fine-particle content - Engineering Geology, 69, pp 109-125.

Wilson, C.J. 1988. Runoff and pore pressures in hollows. PhD Thesis, California University, Berkeley.

Wolle, C.M. & Hachich, W. 1989. Rain-induced landslides in south-eastern Brazil. Proceedings of the 12th Int. Conf. Soil Mech. and Foundation Engineering, vol.3, pp.1639-1644.